Ca^{2+}-Signaling Cycle of a Membrane-Docking C2 Domain†

Eric A. Nalefski, Molly M. Slazas, and Joseph J. Falke*

Department of Chemistry and Biochemistry, University of Colorado at Boulder, Boulder, Colorado 80309-0215

Received July 16, 1997; Revised Manuscript Received August 11, 1997⊗

ABSTRACT: The C2 domain is a Ca^{2+}-dependent, membrane-targeting motif originally discovered in protein kinase C and recently identified in numerous eukaryotic signal-transducing proteins, including cytosolic phospholipase A_2 ($cPLA_2$) of the vertebrate inflammation pathway. Intracellular Ca^{2+} signals recruit the C2 domain of $cPLA_2$ to cellular membranes where the enzymatic domain hydrolyzes specific lipids to release arachidonic acid, thereby initiating the inflammatory response. Equilibrium binding and stopped-flow kinetic experiments reveal that the C2 domain of human $cPLA_2$ binds two Ca^{2+} ions with positive cooperativity, yielding a conformational change and membrane docking. When Ca^{2+} is removed, the two Ca^{2+} ions dissociate rapidly and virtually simultaneously from the isolated domain in solution. In contrast, the Ca^{2+}-binding sites become occluded in the membrane-bound complex such that Ca^{2+} binding and dissociation are slowed. Dissociation of the two Ca^{2+} ions from the membrane-bound domain is an ordered sequential process, and release of the domain from the membrane is simultaneous with dissociation of the second ion. Thus, the Ca^{2+}-signaling cycle of the C2 domain passes through an active, membrane-bound state possessing two occluded Ca^{2+} ions, one of which is essential for maintenance of the protein−membrane complex.

The C2 domain is a widely distributed Ca^{2+}-signaling motif first described in Ca^{2+}- and lipid-dependent isoforms of protein kinase C (*1*−*3*). To date, the membrane-targeted Ca^{2+}-signaling proteins that contain C2 domains comprise at least four functional classes (*4*−*7*): lipid-modifying enzymes, including numerous proteins that generate lipid-derived second messengers; membrane-active protein kinases; proteins that regulate vesicular trafficking; and GTPase-activating proteins. Crystal structures of representative C2 domains from synaptotagmin and phosphoinositide-specific phospholipase C-δ1 have revealed two distinct topologies, type I and type II, that yield strikingly similar tertiary folds (*8*−*13*). Both folds consist of an 8-stranded β-sandwich possessing a Ca^{2+}-binding site formed by interstrand loops at one end of the β-sandwich. Sequence alignments suggest that all known C2 domains exhibit either type I or type II topology (*7*). Because several isolated C2 domains have been shown to bind phospholipids, inositolpolyphosphates, or proteins associated with the membrane, the C2 domain appears to function as a Ca^{2+}-regulated cellular localization motif that controls the docking of signaling proteins to membranes (*7*). This Ca^{2+}-induced membrane targeting is believed to be triggered by the cooperative binding of multiple Ca^{2+} ions (*14*−*16*). However, the stoichiometry of Ca^{2+} binding to the C2 domain remains controversial (*8, 9, 11*−*13*), and key features of the Ca^{2+}-binding equilibrium and kinetics have yet to be determined, particularly for the membrane-bound state.

In cytosolic phospholipase A_2 ($cPLA_2$),[1] and presumably in other Ca^{2+}-activated enzymes regulated by C2 domains, the C2 domain is responsible for recruiting a separate catalytic domain into the vicinity of its membrane-bound substrate (*17, 18*). Thus, the hydrolysis of arachidonyl-containing glycerophospholipids by the $cPLA_2$ phospholipase domain is significantly speeded by the Ca^{2+}-induced docking of the C2 domain to membranes (*19*−*24*). The resulting release of free arachidonic acid leads to the synthesis of leukotrienes and prostaglandins, important mediators of inflammation, cell growth, and differentiation (*25*, *26*). The inflammatory response triggered by $cPLA_2$ is the target of current anti-inflammatory drugs, including aspirin and ibuprofen (*25*).

The $cPLA_2$ C2 domain has been expressed as a separate, independently folded 16 kDa fragment, which reversibly, and selectively, binds phosphatidylcholine vesicles *in vitro* with essentially the same Ca^{2+} dependence as the full-length protein (*56*). The low micromolar Ca^{2+} affinity of this isolated domain is ideally suited for quantitative studies of the Ca^{2+}-binding equilibrium and kinetics, both in the absence and presence of membranes. The present report utilizes the C2 domain of $cPLA_2$ to (i) determine the equilibrium and kinetic parameters for Ca^{2+} binding to a representative C2 domain and (ii) begin to define the sequence of events that occur during Ca^{2+} activation, membrane docking, and complex dissociation.

MATERIALS AND METHODS

Protein Purification. $cPLA_2$ C2 domain (fragment 1−138 of human $cPLA_2$) was expressed in bacterial inclusion bodies as an independent polypeptide by induction of cells carrying the plasmid pTrc-$cPLA_2$(1−138) with β-D-thiogalactopyranoside (*56*). Inclusion body material extracted twice with

† Support provided by NIH Grant GM 48203 (J.J.F.) and NIH Fellowship GM 18303 (E.A.N.).

* Corresponding author. Tel: 303-492-3503. Fax: 303-492-5894. Email: falke@colorado.edu.

⊗ Abstract published in *Advance ACS Abstracts,* September 15, 1997.

[1] Abbreviations: $cPLA_2$, cytosolic phospholipase A_2; Tris, tris(hydroxymethyl)aminomethane; PIPES, piperazine-*N*,*N*′-bis(2-ethanesulfonic acid); EDTA, ethylenediaminetetraacetic acid; SDS, sodium dodecyl sulfate; PAGE, polyacrylamide gel electrophoresis; FRET, fluorescence resonance energy transfer; dansyl-PE, *N*-(5-dimethylaminonapthalene-1-sulfonyl)-*sn*-glycero-3-phosphoethanolamine.

S0006-2960(97)01734-0 CCC: $14.00

chloroform:methanol (2:1) was diluted into refolding buffer composed of 500 mM arginine-HCl, 25 mM tris(hydroxymethyl)aminomethane (Tris), pH 8.0, 5 mM ethylenediaminetetraacetic acid (EDTA), and 5 mM dithiothreitol at 4 °C. After extensive dialysis, properly refolded C2 domain was affinity purified by adsorption to phosphatidylcholine-phenylsepharose resin, prepared as described (*27*), equilibrated in 100 mM KCl, 20 mM Tris, pH 7.8, and 1 mM $CaCl_2$, and elution with the same buffer containing 5 mM EDTA. Purified C2 domain monomers were separated from aggregates by passage over a Sephadex G-75 gel filtration column equilibrated with standard assay buffer [100 mM KCl and 20 mM piperazine-*N*,*N*′-bis(2-ethanesulfonic acid) (PIPES), pH 7.0] containing 1 mM $CaCl_2$. Protein stocks were snap-frozen and stored at −70 °C. Protein solutions were decalcified by passage over Chelex 100 Resin (Bio-Rad Laboratories) prior to use. Purified C2 domain was judged to be >95% pure when analyzed on a sodium dodecyl sulfate polyacrylamide gel electrophoresis (SDS−PAGE) 15% gel. Purified C2 domain exhibited a reversible, Ca^{2+}-dependent shift of electrophoretic mobility when subjected to 15% native PAGE (unpublished experiments).

Phospholipid Vesicle Preparation. Phosphatidylcholine vesicles were prepared by drying chloroform stocks of 1-palmitoyl-2-oleoyl-*sn*-glycero-3-phosphocholine (Avanti Lipids) under a stream of nitrogen, resuspending in standard assay buffer, sonicating to form transparent suspensions of unilamellar vesicles, and decalcification by passage over Chelex resin. For fluorescence resonance energy transfer, *N*-(5-dimethylaminonapthalene-1-sulfonyl)-*sn*-glycero-3-phosphoethanolamine) (dansyl-PE, Molecular Probes) was incorporated into phosphatidylcholine vesicles at 5% (mol/mol).

Equilibrium Dialysis. Equilibrium dialysis was carried out as described previously (*28*) using 3000 molecular weight cut-off dialysis membranes in a microscale equilibrium dialysis apparatus at 22 ± 1 °C. Purified C2 domain (20−30 μM), in the absence or presence of phosphatidylcholine (2 mM) vesicles, was dialyzed against increasing concentrations of $^{45}Ca^{2+}$ in standard assay buffer. After equilibration for 24 h, free and total Ca^{2+} concentrations were determined by scintillation counting, and using the known $^{45}Ca^{2+}$ specific activity, bound Ca^{2+} was calculated by subtraction. These vesicle experiments required no correction for membrane-bound Ca^{2+}, since such binding is calculated to be negligible at the Ca^{2+} levels utilized (*42, 43*), and indeed, no phospholipid-bound $^{45}Ca^{2+}$ was detected in control dialysis experiments lacking the C2 domain. Protein concentrations of samples were determined by Bradford assay (*29*) using a $cPLA_2$ C2 domain standard quantified by the tyrosinate assay (*30*), a method that gave results within 12% of those determined by the protein extinction coefficient (*31*) and bicinchoninic acid assays (*32*) using bovine serum albumin as a standard. Standard errors (represented as error bars in Figure 1A, below) were calculated from errors in protein determination and bound Ca^{2+}. After dialysis, the C2 domain remained monomeric without detectable degradation as judged by native PAGE analysis. Assay buffer and plasticware were decalcified prior to use (*33*).

Equilibrium Fluorescence Spectroscopy. Equilibrium fluorescence experiments were carried out on an SLM 48000S fluorescence spectrometer. C2 domain (0.5 μM), in the presence or absence of phosphatidylcholine (100 μM) vesicles, was titrated with concentrated Ca^{2+} stocks in standard assay buffer at 25 °C. The intrinsic tryptophan fluorescence of Trp^{71} was monitored using excitation and emission wavelengths of λ_{ex} = 284 nm and λ_{em} = 325 nm, with band-pass settings of 4 and 8 nm, respectively. The relative fluorescence increase was calculated as $(I_{obs} - I_{min})/(I_{max} - I_{min})$, where I_{min} represents the intrinsic emission of protein in the absence of Ca^{2+}, I_{obs} denotes the emission at a given free Ca^{2+} concentration, and I_{max} is the maximal emission at saturating Ca^{2+}.

Binding of the C2 domain to membranes was monitored by fluorescence resonance energy transfer (FRET), using Trp^{71} as the donor and dansyl-PE-containing phosphatidylcholine vesicles (see above) as the acceptor. Excitation and emission wavelengths were λ_{ex} = 284 nm and λ_{em} = 520 nm, with band-pass settings of 4 and 8 nm, respectively. Relative FRET was calculated as $(I_{obs} - I_{min})/(I_{max} - I_{min})$, where I_{min} represents the dansyl emission of vesicles and protein in the absence of Ca^{2+}.

When analyzing Ca^{2+} titrations, by either intrinsic tryptophan fluorescence or FRET, the free Ca^{2+} concentration was calculated by correcting the total for the small fraction of Ca^{2+} bound to the C2 domain (Table 1, below). Binding of Ca^{2+} to the phosphatidylcholine membranes was negligible as determined from the known K_D (*42, 43*) and equilibrium dialysis. In FRET experiments measuring the K_D of phosphatidylcholine, the concentration of C2 domain was small compared to the lipid concentration; thus, the free lipid concentration was assumed to equal the total concentration.

Stopped-Flow Fluorescence Spectroscopy. Stopped-flow fluorescence spectroscopy was carried out as described (*34, 35*) on an Applied Photophysics model 17MV stopped-flow apparatus using standard assay buffer at 25 °C. The dead time of the apparatus was determined to be 1.0 ms (*36*). To monitor Ca^{2+} release, a suspension of 5 μM C2 domain in 100 μM Ca^{2+}, with or without freshly prepared phosphatidylcholine (250 μM) vesicles, was rapidly mixed with 150 μM Quin-2 (Molecular Probes), a fluorescent chelator (*37*). The Quin-2 excitation wavelength was λ_{ex} = 332 nm, and emission was detected using a 490 nm band-pass filter. The amplitude of the Quin-2 fluorescence signal was converted to concentration of released Ca^{2+} ions using a Quin-2 fluorescence standard curve generated by mixing Quin-2 with known concentrations of Ca^{2+}. This concentration was then converted to the stoichiometry of Ca^{2+} released per C2 domain using the known protein concentration (see above). To monitor conformational changes in the C2 domain triggered by Ca^{2+} release, a suspension containing 5 μM C2 domain in 100 μM Ca^{2+}, with or without phosphatidylcholine (250 μM) vesicles, was rapidly mixed with 5 mM EDTA. The intrinsic Trp^{71} fluorescence was excited at λ_{ex} = 284 nm and detected using a 335 nm high-pass filter. The resulting fluorescence signal was normalized to the total fluorescence change. To monitor changes in the protein-to-membrane FRET triggered by Ca^{2+} release, a suspension of 5 μM C2 domain in 100 μM Ca^{2+} and phosphatidylcholine (250 μM) vesicles containing dansyl-PE was rapidly mixed with 5 mM EDTA. The FRET was excited at λ_{ex} = 284 nm and detected using a 475 nm high-pass filter. A total of 4000 data points were collected over a period of 5 s for slow dissociation processes and over 250 ms for rapid processes. In all stopped-flow experiments, five transients were collected and averaged on at least three separate occasions.

Data Analysis. Equilibrium dialysis data were plotted as the number of Ca^{2+} ions bound per C2 domain (y) versus free Ca^{2+} (x) and then were fitted to standard equations describing different binding models (*38*) utilizing KaleidaGraph software (Version 3.08, Synergy Software, 1996). The Ca^{2+}-binding models tested and their independently varying parameters were (a) homogenous population of single independent sites (eq 1, n, K_D); (b) two independent sites (eq 2: n, K_{D1}, K_{D2}); (c) cooperative sites in the Hill model [eq 3, n, K_D, H (Hill coefficient)]; and (d) two cooperative sites in the sequential model (eq 4, n, K_{D1}, K_{D2}):

$$y = n\left(\frac{x}{K_D + x}\right) \quad (1)$$

$$y = \frac{n}{2}\left(\frac{x}{K_{D1} + x} + \frac{x}{K_{D2} + x}\right) \quad (2)$$

$$y = n\left(\frac{x^H}{K_D{}^H + x^H}\right) \quad (3)$$

$$y = \frac{n}{2}\left(\frac{xK_{D2} + 2x^2}{K_{D1}K_{D2} + xK_{D2} + x^2}\right) \quad (4)$$

where K_D represents the macroscopic equilibrium dissociation constant and the stoichiometric normalization constant (n) was used to calculate Ca^{2+}-binding stoichiometries (in moles of Ca^{2+} bound per moles of C2 domain). The χ^2 values obtained using the Hill and sequential models were less than half those obtained using independent one- or two-site models (data not shown), demonstrating the superior fit provided by the cooperative models.

Equilibrium tryptophan or FRET fluorescence data were plotted as the relative fluorescence signal (y) versus free Ca^{2+} (x) and fitted to the Hill equation (experiments involving Ca^{2+} titrations) or single independent-site equation (experiments involving phospholipid titrations). It is important to note that although the Ca^{2+} titrations of Trp^{71} fluorescence and protein-to-membrane FRET can be well-fit by cooperative binding equations, the resulting best-fit parameters are not directly comparable to those obtained for direct Ca^{2+}-binding measurements because the two Ca^{2+}-binding events may trigger different fluorescence or FRET changes. As a result, the slope of the fluorescence profile depends on the relative magnitudes of the fluorescence changes for the two Ca^{2+} binding events (*39*).

Stopped-flow data were plotted as the fluorescence signal (F) versus time (t) and analyzed by best-fitting to single or double exponential functions (*40*, *41*) in which independent parameters were allowed to float. The single exponential function, which represents a first-order process in which two Ca^{2+} ions dissociate virtually simultaneously from the C2 domain (P), is described by eq 5:

$$F(t) = \Delta F\,(1 - e^{-kt}) + C \quad (5)$$

where k is the rate constant of the event monitored, ΔF is the fluorescence amplitude, and C is the intrinsic voltage offset of the stopped-flow experiment. The double exponential function, representing the ordered sequential dissociation of two Ca^{2+} ions from a pair of coupled sites (*41*), is described by eq 6:

$$F(t) = (\Delta F_1 + \Delta F_2) \times \left[1 + \left(\frac{\Delta F_1}{\Delta F_1 + \Delta F_2}\,\frac{k_1}{k_2 - k_1} - \frac{k_2}{k_2 - k_1}\right)e^{-k_1 t} - \left(\frac{\Delta F_1}{\Delta F_1 + \Delta F_2}\,\frac{k_1}{k_2 - k_1} - \frac{k_1}{k_2 - k_1}\right)e^{-k_2 t}\right] + C \quad (6)$$

where k_1 and k_2 are the rate constants of the first and second ordered events, respectively, and where ΔF_1 and ΔF_2 are the fluorescence amplitudes of these steps. For Ca^{2+} dissociation from the isolated domain, the monophasic time course calculated from eq 5 provided the optimal fit. In contrast, Ca^{2+} dissociation from the membrane-bound domain was poorly fit by the monoexponential function but was optimally fit by the biphasic time course calculated from eq 6. The latter biphasic time course was not as well approximated by a two independent site model in which the two exponential terms have equal weights. Moreover, the biphasic behavior was not a result of material heterogeneity in the protein−membrane complexes since the same two kinetic phases were consistently observed in samples prepared from different lots of protein and membranes, or at different saturating concentrations of these components. Thus, the Ca^{2+} dissociation time courses of the isolated and membrane-bound domains are optimally fit by (i) simultaneous and (ii) ordered sequential dissociation models, respectively.

RESULTS

Equilibrium Ca^{2+} Binding. To directly measure the equilibrium affinity and stoichiometry of Ca^{2+} binding to the $cPLA_2$ C2 domain, equilibrium $^{45}Ca^{2+}$ dialysis experiments were carried out in the absence and presence of phosphatidylcholine vesicles (Figure 1A). The resulting Ca^{2+}-binding curves were analyzed by the method of nonlinear least-squares in terms of different binding models (see Materials and Methods, eqs 1−4). Single-site and independent two-site models (eqs 1 and 2) failed to adequately fit the data, but optimal fits were obtained for cooperative models using either the Hill or the sequential binding equations (eqs 3 and 4), the results of which are summarized in Table 1. The resulting best-fit stoichiometries indicate that the C2 domain binds two Ca^{2+} ions in both its isolated and membrane-bound states (Table 1). In the absence of membranes, the Hill model shows that the two Ca^{2+} ions bind with positive cooperativity (Hill coefficient of 1.4), yielding a macroscopic equilibrium dissociation constant (K_D) of 24 μM. Positive cooperativity is also revealed by the two-site sequential model, which describes the stoichiometric binding of two Ca^{2+} ions to the domain (P):

$$P + 2Ca \overset{K_1}{\rightleftharpoons} P{\cdot}Ca + Ca \overset{K_2}{\rightleftharpoons} P{\cdot}Ca_2 \quad (7)$$

where the stoichiometric binding constant (K_n) is the inverse of the stoichiometric dissociation constant (K_{Dn}). In this picture, the second stoichiometric binding event exhibits a higher macroscopic affinity (K_{D2} of 10 μM) than the first stoichiometric event (K_{D1} of 56 μM). In the presence of saturating phosphatidylcholine vesicles, the two Ca^{2+}-binding sites retain significant positive cooperativity, but the Ca^{2+} affinity is increased approximately 8-fold (Table 1).

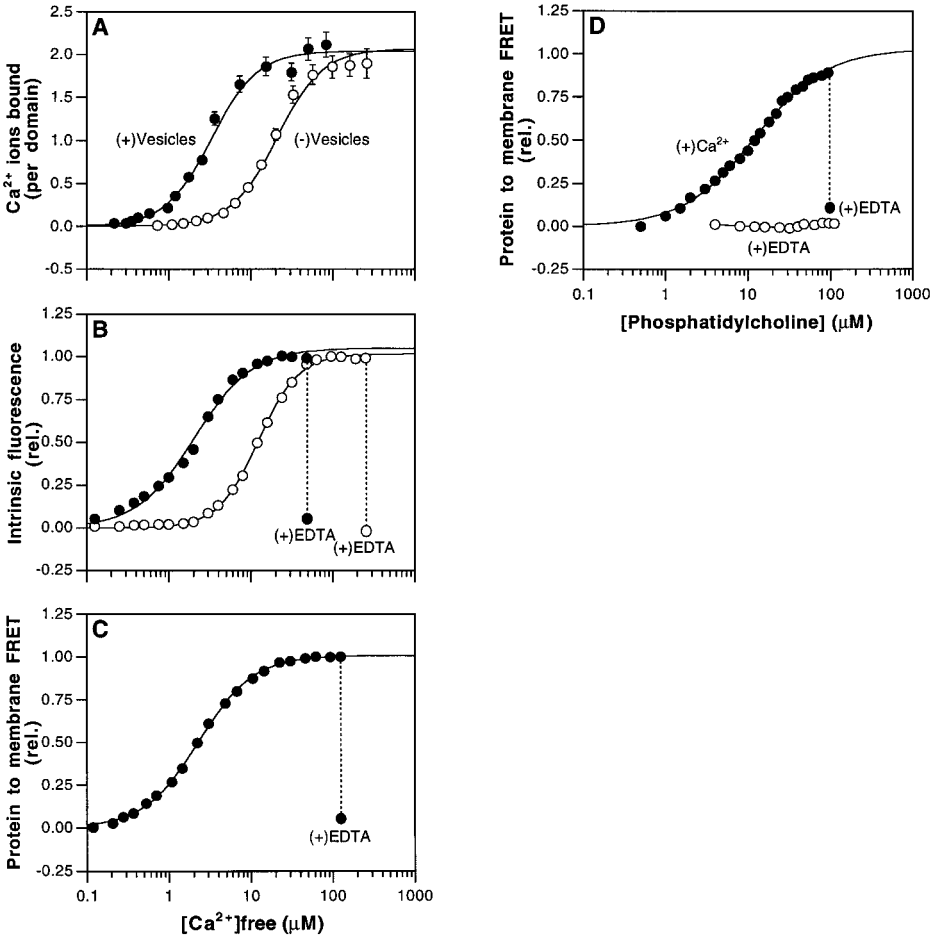

FIGURE 1: Equilibrium Ca^{2+} and membrane binding to the $cPLA_2$ C2 domain. (A) Binding of $^{45}Ca^{2+}$ to the isolated $cPLA_2$ C2 domain in the absence (open symbols) or presence (closed symbols) of phosphatidylcholine vesicles, as measured by equilibrium dialysis. Solid curves indicate the best-fit by the Hill model (eq 3), yielding the binding parameters summarized in Table 1. Experimental conditions: 100 mM KCl, 20 mM PIPES, pH 7.0; 20 μM C2 domain with or without 2 mM phosphatidylcholine; 22 ± 1 °C. (B) Ca^{2+}-induced conformational changes in the absence (open symbols) or presence (closed symbols) of phosphatidylcholine vesicles, as detected by the intrinsic Trp^{71} fluorescence. Solid curves indicate the best-fit by the Hill equation. Average (±SEM) $[Ca^{2+}]_{1/2}$ values obtained were 13 ± 1 μM and 2.2 ± 0.1 μM in the absence and presence of vesicles, respectively ($n = 3$). The Ca^{2+}-induced fluorescence increases were fully reversed by the addition of excess Ca^{2+} chelator EDTA, as indicated by the dashed lines. Experimental conditions: same as panel A except 0.5 μM C2 domain with or without 100 μM phosphatidylcholine; T = 25 °C. (C) Binding of the C2 domain to phosphatidylcholine vesicles as revealed by FRET from Trp^{71} of the $cPLA_2$ C2 domain to dansylated headgroups. The solid curve represents the best-fit of data by the Hill equation. The average (±SEM) $[Ca^{2+}]_{1/2}$ value obtained was 3.3 ± 0.4 μM ($n = 3$). The Ca^{2+}-induced membrane binding was fully reversed by the addition of excess EDTA, as indicated by the dashed line. Experimental conditions same as panel B. (D) Net phospholipid dependence of membrane binding by the C2 domain was determined in the absence or presence of bound Ca^{2+} ion. The Ca^{2+}-saturated (filled symbols) and Ca^{2+}-free (open symbols) states were maintained with 1 mM EDTA plus 2 mM $CaCl_2$ or with 1 mM EDTA, respectively. Parallel control titrations were carried out with no protein, thereby providing the FRET baseline. The solid curve represents the best-fit of data to a homogeneous population of independent sites (eq 1). The average (±SEM) apparent K_D value obtained for phosphatidylcholine binding was 10 ± 2 μM in the presence of saturating Ca^{2+} ($n = 5$). Membrane binding was reversed by the addition of excess EDTA, as indicated by the dashed line. Experimental conditions same as panel B.

Table 1: Equilibrium Ca^{2+}-Binding Parameters of the $cPLA_2$ C2 Domain[a]

	Hill model			two-site sequential model		
treatment	K_D (μM)	Hill coefficient	stoichiometry (mol/mol)	K_{D1} (μM)	K_{D2} (μM)	stoichiometry (mol/mol)
− vesicles	24 ± 2	1.4 ± 0.1	1.9 ± 0.1	60 ± 10	10 ± 4	1.7 ± 0.1
+ vesicles	3.1 ± 0.4	1.5 ± 0.1	1.8 ± 0.1	7 ± 1	1.5 ± 0.7	1.8 ± 0.1

[a] Ca^{2+} binding to the C2 domain in the absence (−) or presence (+) of phosphatidylcholine vesicles was determined by equilibrium $^{45}Ca^{2+}$ dialysis at 22 ± 1 °C in 100 mM KCl, 20 mM PIPES, pH 7.0. Data were analyzed by best-fit to the Hill equation and the two-site sequential binding models (eqs 3 and 4, respectively). Results are represented as means (±SEM) of three independent determinations. Stoichiometry is reported as moles of Ca^{2+} bound per mole of C2 domain.

Ca^{2+}-Induced Conformational Change. Evidence that Ca^{2+} binding and membrane docking trigger conformational changes in the C2 domain was provided by monitoring changes in the intrinsic fluorescence of the single tryptophan Trp^{71} of the $cPLA_2$ C2 domain (Figure 1B). Binding of Ca^{2+} to the domain increased the Trp^{71} fluorescence by as much as 15% in the absence of phosphatidylcholine vesicles and 30% in the presence of vesicles. It follows that Trp^{71} is sensitive to conformational changes associated with both Ca^{2+} binding and membrane docking. The Ca^{2+} dependence

of the Trp^{71} fluorescence is quite similar to the Ca^{2+}-binding curve obtained by equilibrium dialysis; noteably, these two disparate methods yielded $[Ca^{2+}]_{1/2}$ values that agreed within 2-fold both in the absence and presence of vesicles (Figure 1, panels A and B). The Ca^{2+}-dependent fluorescence increase in Trp^{71} was completely reversed by addition of excess EDTA.

Ca^{2+}-Induced Membrane Docking. The Ca^{2+}-triggered docking of the $cPLA_2$ C2 domain to phosphatidylcholine vesicles was directly monitored by a fluorescence resonance energy transfer (FRET) assay (Figure 1C). This experiment utilizes Trp^{71} as the fluorescence donor and dansyl-labeled headgroups on the surface of phosphatidylcholine vesicles as acceptors so that energy transfer is observed only when the C2 domain is bound to the membrane. Titration of the FRET signal with Ca^{2+} yielded the same Ca^{2+} dependence, within error, as that observed for Ca^{2+} binding to the domain in the presence of membranes (Figure 1, panels A and C). This Ca^{2+}-induced protein-to-membrane FRET was completely reversed by addition of excess EDTA.

The FRET assay also enabled determination of the lipid dependence of Ca^{2+}-triggered membrane docking (Figure 1D). In the absence of Ca^{2+}, the C2 domain displayed no measurable binding to vesicles at phosphatidylcholine concentrations up to 100 μM. In contrast, binding of the Ca^{2+}-occupied C2 domain to phosphatidylcholine vesicles saturated as the phospholipid concentration was raised, yielding half-maximal FRET at a phosphatidylcholine concentration of 10 μM. Addition of excess EDTA quantitatively disrupted the protein−membrane complex, thereby demonstrating the reversibility of the Ca^{2+}-triggered docking reaction. Thus, Ca^{2+} induces over a 10-fold enhancement in the affinity of the C2 domain for target membrane vesicles. Separate experiments have shown that the $cPLA_2$ C2 domain selectively binds choline in preference to other headgroups (*56*).

Kinetics of Ca^{2+} Dissociation. Overall, the equilibrium studies of the $cPLA_2$ C2 domain demonstrate the existence of two positively cooperative Ca^{2+}-binding sites that are directly linked to intradomain conformational changes. The same two sites are also responsible for driving headgroup-specific membrane docking. Kinetic studies of Ca^{2+} dissociation were initiated to independently test the two-site cooperative Ca^{2+}-binding model and to examine the sequence of events during the inactivation of the $(Ca^{2+})_2$−protein−membrane complex.

Ca^{2+} dissociation experiments were carried out in a stopped-flow fluorescence spectrometer using the fluorescent Ca^{2+}-chelator Quin-2 to detect and trap Ca^{2+} released from the Ca^{2+}-loaded C2 domain (Figure 2A). The resulting Ca^{2+}-dissociation time courses were analyzed by best-fitting to single or double exponential functions. In the absence of membranes, Ca^{2+} dissociation from the C2 domain was optimally fit by the monoexponential time course (eq 5) of a simultaneous dissociation model:

$$P{\cdot}Ca_2 \xrightarrow[\Delta F]{k} P + 2Ca \qquad (8)$$

where k is the rate constant and ΔF is the maximal fluorescence change. Best fitting of the data by this single exponential model (Figure 2A) revealed a Ca^{2+} dissociation rate constant of 111 s^{-1} (Table 2). The Quin-2 fluorescent change (ΔF) was converted to a stoichiometry, indicating that 1.9 ions are released per domain, independently confirming the two-site binding observed in equilibrium experiments.

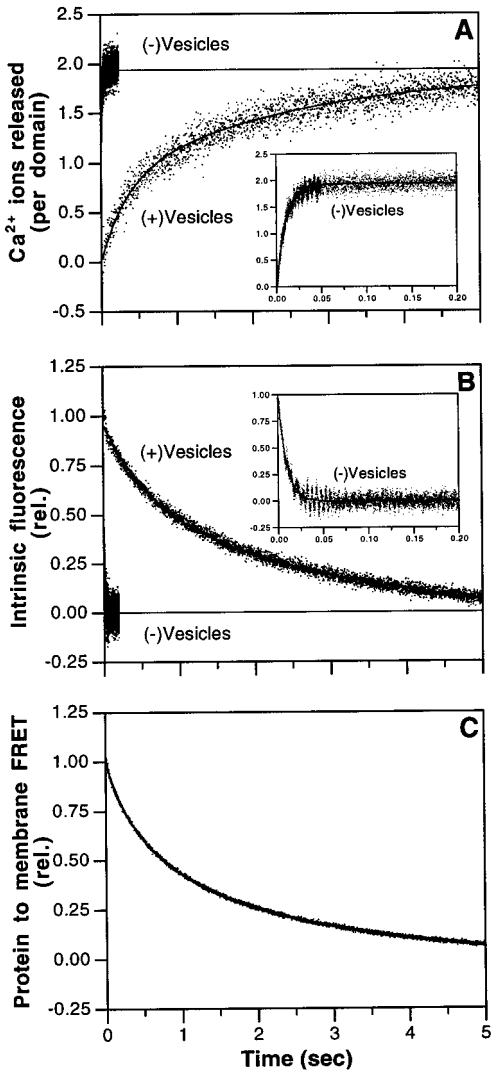

FIGURE 2: Kinetics of Ca^{2+} dissociation and accompanying events measured for the $cPLA_2$ C2 domain by stopped-flow fluorescence. (A) Dissociation of Ca^{2+} from the $cPLA_2$ C2 domain in the absence or presence of phosphatidylcholine vesicles. The time course was triggered by rapidly mixing with the fluorescent Ca^{2+} indicator Quin-2, and the resulting Quin-2 fluorescence signal was converted to the concentration of Ca^{2+} ions for stoichiometry determination. Best-fit solid curves were generated for the simultaneous (eq 5) and ordered sequential (eq 6) dissociation models in the absence or presence of vesicles, respectively, yielding the dissociation parameters summarized in Table 2. (B) Conformational changes triggered by Ca^{2+} removal from the C2 domain in the absence or presence of phosphatidylcholine vesicles. The domain conformation was monitored using the intrinsic fluorescence Trp^{71} following rapid mixing with excess EDTA. Best-fit solid curves were generated as in panel a, yielding the dissociation parameters summarized in Table 2. (C) Conformational rearrangements and membrane release of the C2 domain, as revealed by protein-to-membrane FRET. The time course was triggered by rapid mixing of Ca^{2+}-saturated C2 domain with excess EDTA. The solid curve represents the best-fit analysis by the ordered sequential dissociation model (eq 6), yielding the dissociation parameters summarized in Table 2. Experimental conditions in panels a−c: 100 mM KCl, 20 mM PIPES, pH 7.0; 5 μM C2 domain with or without 250 μM phosphatidylcholine; 25 °C.

In the presence of saturating concentrations of phosphatidylcholine vesicles, Ca^{2+} dissociation from the C2 domain

Table 2: Kinetic Parameters for Events Triggered by Ca^{2+} Dissociation from the $cPLA_2$ C2 Domain[a]

	Ca^{2+} dissociation[b]		conformational change[c]		protein-to-membrane FRET[d]	
treatment	k_{off} (s^{-1})	stoichiometry (mol/mol)	k (s^{-1})	ΔF (rel)	k (s^{-1})	ΔF (rel)
− vesicles[e]	111 ± 3	1.88 ± 0.03	112 ± 1			
+ vesicles[f]						
step 1	5.5 ± 0.3	1.0 ± 0.1	3.2 ± 0.2	0.38 ± 0.01	3.1 ± 0.1	0.40 ± 0.03
step 2	0.53 ± 0.01	1.01 ± 0.03	0.45 ± 0.01	0.62 ± 0.01	0.52 ± 0.01	0.60 ± 0.03

[a] Kinetic parameters for events triggered by Ca^{2+} dissociation from the $cPLA_2$ C2 domain expressed as averages (±SEM) for n experiments determined by stopped-flow fluorescence spectroscopy at 25 °C in 100 mM KCl, 20 mM PIPES, pH 7.0. [b] The fluorescent Ca^{2+} chelator Quin-2 was used to monitor dissociation of Ca^{2+} ions from the C2 domain in the absence ($n = 15$) or presence ($n = 19$) of phosphatidylcholine vesicles. Stoichiometry is reported as moles of Ca^{2+} bound per moles of C2 domain. [c] The intrinsic Trp^{71} fluorescence of the C2 domain was used to monitor Ca^{2+} dissociation-induced conformational changes in the C2 domain in the absence ($n = 4$) or presence ($n = 11$) of vesicles. [d] Protein-to-membrane FRET was used to monitor Ca^{2+} dissociation-induced conformational changes and the breakdown of the $(Ca^{2+})_2$−C2−membrane complex ($n = 9$). [e] Determined from best-fit of a single exponential function for simultaneous dissociation (eq 5). [f] Determined from best-fit of a double exponential function for ordered sequential dissociation (eq 6).

(Figure 2A) was poorly fit by a single exponential function (eq 5, data not shown). Rather, the time course contained two kinetically resolvable phases and was optimally fit by the double exponential function (eq 6) of an ordered sequential dissociation model:

$$P{\cdot}Ca_a{\cdot}Ca_b \xrightarrow[\Delta F_1]{k_1} P{\cdot}Ca_b + Ca \xrightarrow[\Delta F_2]{k_2} P + 2Ca \qquad (9)$$

where the Ca^{2+} ion bound to site "a" (Ca_a) is always released before the ion bound to "b" (Ca_b).

This ordered sequential dissociation was consistent with the strong intersite positive cooperativity observed in equilibrium Ca^{2+} binding experiments (Table 1). By contrast, the sequential dissociation could not be accounted for by two independent sites or by heterogeneity of protein−membrane complexes (see Materials and Methods). Best fitting of the data by the ordered sequential model (Figure 2A) yielded rates of 5.5 s^{-1} and 0.53 s^{-1} for the first and second Ca^{2+} dissociation events, respectively (Table 2). The fluorescence amplitudes of these two events were the same, within error, and yielded Ca^{2+} stoichiometries of 1.0 per dissociation event as expected for a pair of cooperative sites.

Thus, as observed for equilibrium Ca^{2+} binding, the Ca^{2+} dissociation time courses of isolated or membrane-bound C2 domains reveal two Ca^{2+}-binding sites per domain. The membrane-bound domain exhibits ordered sequential dissociation of the two Ca^{2+} ions (eq 9), such that the first Ca^{2+} dissociates 10-fold more rapidly than the second, in contrast to the isolated domain where the two ions dissociate virtually simultaneously (eq 8).

Kinetics of Events Accompanying Ca^{2+} Dissociation. The time courses of events triggered by Ca^{2+} dissociation were observed in stopped-flow experiments in which the intrinsic tryptophan fluorescence or protein-to-membrane FRET was monitored (Figure 2, panels B and C). Rapid mixing of Ca^{2+}-loaded C2 domain with EDTA in the absence of membranes generated a Trp^{71} fluorescence time course that was optimally fit by a single exponential function (eq 5). It follows that the virtually simultaneous release of both Ca^{2+} ions observed under these conditions (see above) is accompanied by a conformational change within the domain. Dissociation of Ca^{2+} from the membrane-bound complex, by contrast, yielded a biphasic decay of Trp^{71} fluorescence that was optimally fit by the double exponential kinetics of an ordered sequential process (eq 6). The resulting ordered rate constants k_1 and k_2 for the intrinsic fluorescence changes were similar to those observed for Ca^{2+} dissociation (Table 2), indicating that the stepwise Ca^{2+} dissociation alters the conformation of the membrane-bound C2 domain in two distinct stages. In the energy transfer experiment, the decay of protein-to-membrane FRET following rapid mixing with EDTA yielded essentially the same ordered sequential rate constants k_1 and k_2 observed for the Trp^{71} fluorescence change (Table 2). It follows that the Trp^{71} fluorescence decrease triggered by the first Ca^{2+}-dissociation event elicits a partial loss of FRET. Subsequently, the remaining FRET is lost when the second Ca^{2+} dissociates and the protein−membrane complex falls apart.

DISCUSSION

The results presented here indicate that the $cPLA_2$ C2 domain binds two Ca^{2+} ions in the absence or presence of phosphatidylcholine vesicles. The Ca^{2+}-activation threshold of the isolated domain ($[Ca^{2+}]_{1/2} \approx 20\ \mu M$) is too high to provide full activation by cellular Ca^{2+} signals. In the presence of saturating membranes, however, the activation threshold is lowered by membranes approximately 8-fold ($[Ca^{2+}]_{1/2} \approx 3\ \mu M$) into the range of Ca^{2+} concentrations generated by intracellular Ca^{2+} fluxes (*44*−*47*). Analogously, as expected from thermodynamic coupling, saturating levels of Ca^{2+} substantially increase the affinity of phospholipid binding. Ca^{2+}-induced conformational changes detected by monitoring the intrinsic fluorescence of the C2 domain indicate a direct link between Ca^{2+} binding and protein conformational changes in the vicinity of Trp^{71}. This conformational coupling is likely to extend at least 12 Å, which is the distance between the Ca^{2+}-binding site and the corresponding tryptophan side chain in the related C2 domain of phosphoinositide-specific phospholipase C-δ1 (*10*, *11*, *13*). The striking similarities between the Ca^{2+} dependences of Ca^{2+} binding, conformational changes, and membrane docking suggest that all of these events are coupled.

Further, the results indicate that two Ca^{2+} ions dissociate essentially simultanously from the isolated C2 domain. Similarly, EF-hand Ca^{2+}-binding domains, which also possess a pair of positively cooperative Ca^{2+}-binding sites, typically release both Ca^{2+} ions virtually simultaneously (*48*, *49*). Although such positively cooperative pairs of sites are expected to release their Ca^{2+} in a sequential fashion, it is common for the time course to appear monophasic because the second event is too fast to resolve. This behavior is explained by examination of the kinetic equation describing ordered sequential dissociation (eq 6) which, in the limit of very rapid dissociation from the second site ($k_2 \gg k_1$), reduces

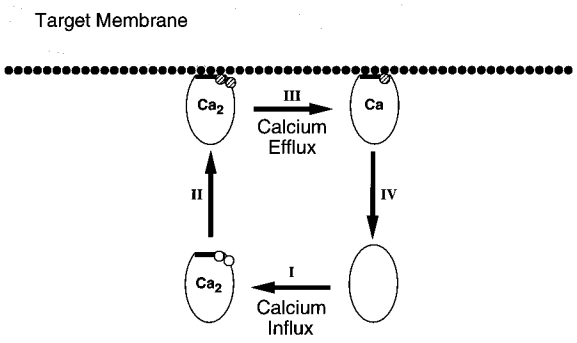

FIGURE 3: Model for events during Ca^{2+}-regulated membrane binding and dissociation. During an intracellular Ca^{2+} signal (step I) two Ca^{2+} ions (circles) bind cooperatively to the C2 domain, triggering conformational changes within the domain as well as docking to a target cytoplasmic membrane (step II). The two Ca^{2+} ions in this protein−membrane complex are occluded, as indicated by hatching. Rapid removal of free Ca^{2+} (step III) triggers a sequential Ca^{2+} dissociation (steps III and IV), in which the loss of the second ion is simultaneous with the dissociation of the protein from the membrane (step IV).

to the same monophasic equation derived for simultaneous dissociation (eq 5). In contrast to the simultaneous dissociation of two Ca^{2+} ions from the isolated domain, the two Ca^{2+} ions dissociate in a strikingly biphasic manner from the membrane-bound C2 domain. The resulting time course represents the strongest example of sequential Ca^{2+} dissociation observed to date. A more subtle ordered sequential time course has been previously observed for Ca^{2+} dissociation from the coupled EF-hand sites of whiting parvalbumin (*41*).

The dissociation of the two Ca^{2+} ions triggers conformational changes within the C2 domain and, ultimately, release from the membrane. For the isolated domain, a single conformational change is observed on the same timescale as the simultaneous release of the two Ca^{2+} ions. For the membrane-bound domain, two sequential conformational changes are observed, corresponding to stepwise Ca^{2+} release. In protein-to-membrane FRET experiments, the conformational change triggered by the first Ca^{2+} release event is found to alter FRET, whereas the remaining FRET is lost when the second Ca^{2+} dissociates. It follows that the second Ca^{2+}-dissociation event is simultaneous with the breakdown of the protein−membrane complex. It is important to note that well after the first Ca^{2+} dissociates, the domain remains bound to the membrane until the second Ca^{2+} is released. Thus, the latter slowly dissociating Ca^{2+} ion is sufficient to maintain the membrane-bound state, at least transiently.

Taken together, these results are consistent with the cycle of Ca^{2+} activation and inactivation presented in Figure 3. In resting cells, the $cPLA_2$ C2 domain is free in the cytosol in its apo-Ca^{2+} state. During a cytoplasmic Ca^{2+} flux, the C2 domain binds two Ca^{2+} ions with positive cooperativity, indicating that the binding of the first Ca^{2+} ion organizes the site to favor binding of a second Ca^{2+}. The resulting cooperative Ca^{2+} binding increases the steepness of the Ca^{2+}-activation threshold, yielding enhanced sensitivity to small changes in cellular Ca^{2+} levels. The binding of two Ca^{2+} ions also induces intradomain conformational changes and drives the membrane interaction, yielding a $(Ca^{2+})_2$−protein−membrane complex. Significantly, in this membrane-bound complex, the Ca^{2+} off-rate is 20−200-fold slower than that of the free domain whereas the macroscopic Ca^{2+} affinity is increased only 8-fold. It follows that both the Ca^{2+} on- and off-rates are significantly slowed by membrane association. Thus, the two Ca^{2+}-binding sites are substantially occluded in the membrane-bound state, either by the membrane itself or by a membrane-induced conformational change. A simple model postulates that one or both Ca^{2+} ions are coordinated by phospholipid headgroups, as proposed for the unrelated proteins annexin V (*50*) and secreted PLA_2 (*51*, *52*), which would directly account for the observed Ca^{2+} occlusion and enhanced Ca^{2+} affinity of the C2 domain in the presence of membranes. Currently, however, the results do not rule out the possibility that Ca^{2+} binding may induce a conformational change elsewhere in the C2 domain to create a phospholipid-binding surface, as has been demonstrated for the EF-hand protein recoverin, in which Ca^{2+} binding induces exposure of a distinct membrane insertion moiety (*53*−*55*). Upon removal of Ca^{2+} from the system, which mimics the end of a rapid intracellular Ca^{2+} signal, the two Ca^{2+} ions dissociate from the membrane-bound domain via an ordered sequential process. Since the departure of the C2 domain from the membrane is approximately simultaneous with the loss of the second Ca^{2+} ion, the second ion is more critical than the first to the kinetic stability of the membrane-bound state.

The available results further indicate that this model of the Ca^{2+}-signaling cycle is likely to be generalizable to other C2 domains. Structural studies are consistent with the binding of two Ca^{2+} ions to C2 domains from synaptotagmin, protein kinase C, and phospholipase C-δ1 (*8*−*11*,*13*). Still other C2 domains exhibit steep Ca^{2+}-dependent activation profiles that can be interpreted as arising from pairs of cooperative sites (*14*−*16*). Thus, the available evidence is consistent with the proposal that Ca^{2+}-regulated C2 domains typically bind two Ca^{2+} ions with positive cooperativity prior to membrane binding, although it would not be surprising to find variant C2 domains with atypical Ca^{2+} binding stoichiometries and cooperativities that are highly specialized for certain signaling applications. The Ca^{2+}-induced conformational change exhibited by the $cPLA_2$ C2 domain may also be widespread in C2 domains, since conformational changes observed in C2 domains from synaptotagmin (*8*) and phospholipase C-δ1 (*11*) may represent homologous Ca^{2+}-triggered structural rearrangments. Further studies are needed to confirm the generality of the two-Ca^{2+}-binding motif and to ascertain the mechanism of Ca^{2+}-induced membrane docking.

ACKNOWLEDGMENT

The authors thank Drs. T. Cech, J. Clark, and O. Peersen for helpful discussions and insightful comments on the manuscript.

REFERENCES

1. Coussens, L., Parker, P. J., Rhee, L., Yang-Feng, T. L., Chen, E., Waterfield, M. D., Francke, U., and Ullrich, A. (1986) *Science 233*, 859.
2. Nishizuka, Y. (1988) *Nature 334*, 661.
3. Newton, A. C. (1995) *Curr. Biol. 5*, 973.
4. Clark, J. D., Schievella, A. R., Nalefski, E. A., and Lin, L.-L. (1995) *J. Lipid Mediators Cell Signalling 12*, 83.
5. Brose, N., Hofmann, K., Hata, Y., and Südhof, T. C. (1995) *J. Biol. Chem. 270*, 25273.
6. Ponting, C. P., and Parker, P. J. (1996) *Protein Sci. 5*, 162.
7. Nalefski, E. A., and Falke, J. J. (1996) *Protein Sci. 5*, 2375.

8. Sutton, R. B., Davletov, B. A., Berghuis, A. M., Südhof, T. C., and Sprang, S. R. (1995) *Cell 80*, 929.
9. Shao, X., Davletov, B. A., Sutton, R. B., Südhof, T. C., and Rizo, J. (1996) *Science 273*, 248.
10. Essen, L.-O., Perisic, O., Katan, M., and Williams, R. L. (1996) *Nature 380*, 595.
11. Grobler, J. A., Essen, L.-O., Williams, R. L., and Hurley, J. H. (1996) *Nat. Struct. Biol. 3*, 788.
12. Grobler, J. A., and Hurley, J. H. (1997) *Nat. Struct. Biol. 4*, 261.
13. Essen, L.-O., Perisic, O., Lynch, D. E., Katan, M., and Williams, R. L. (1997) *Biochemistry 36*, 2753.
14. Davletov, B. A., and Südhof, T. C. (1993) *J. Biol. Chem. 268*, 26386.
15. Li, C., Davletov, B. A., and Südhof, T. C. (1995) *J. Biol. Chem. 270*, 24898.
16. Fukuda, M., Kojima, T., and Mikoshiba, K. (1996) *J. Biol. Chem. 271*, 8430.
17. Clark, J. D., Lin, L.-L., Kriz, R. W., Ramesha, C. S., Sultzman, L. A., Lin, A. Y., Milona, N., and Knopf, J. L. (1991) *Cell 65*, 1043.
18. Nalefski, E. A., Sultzman, L. A., Martin, D. M., Kriz, R. W., Towler, P. S., Knopf, J. L., and Clark, J. D. (1994) *J. Biol. Chem. 269*, 18239.
19. Leslie, C. C., Voelker, D. R., Channon, J. Y., Wall, M. M., and Zelarney, P. T. (1988) *Biochim. Biophys. Acta 963*, 476.
20. Clark, J. D., Milona, N., and Knopf, J. L. (1990) *Proc. Natl. Acad. Sci. U.S.A. 87*, 7708.
21. Gronich, J. H., Bonventre, J. V., and Nemonoff, R. A. (1990) *J. Biol. Chem. 271*, 37.
22. Kramer, R. M., Roberts, E. F., Manetta, J. V., Hyslop, P. A., and Jakubowski, J. A. (1991) *J. Biol. Chem. 266*, 5268.
23. Takayama, K., Kudo, I., Kim, D. K., Nagata, K., Nozawa, T., and Inoue, K. (1991) *FEBS Lett. 282*, 326.
24. Wijkander, J., and Sundler, R. (1991) *Eur. J. Biochem. 202*, 873.
25. Samuelsson, B., Dahlen, S. E., Lindgren, J. A., Rouzer, C. A., and Serhan, C. N. (1987) *Science 237*, 1171.
26. Irvine, R. F. (1982) *Biochem. J. 204*, 3.
27. Evans, T. C., and Nelsestuen, G. L. (1994) *Biochemistry 33*, 13231.
28. Synder, E. E., Buoscio, B. B., and Falke, J. J. (1990) *Biochemistry 29*, 3937.
29. Bradford, M. M. (1976) *Anal. Biochem. 72*, 248.
30. Copeland, R. A. (1994) *Methods for Protein Analysis*, Chapman and Hall, New York.
31. Gill, S. C., and von Hippel, P. H. (1989) *Anal. Biochem. 182*, 319.
32. Smith, P. K., Krohn, R. I., Hermanson, G. T., Mallia, A. K., Gartner, F. H., Provenzano, M. D., Fujimoto, E. K., Goeke, N. M., Olson, B. J., and Klenk, D. C. (1985) *Anal. Biochem. 150*, 76.
33. Needham, J. V., Chen, T. Y., and Falke, J. J. (1993) *Biochemistry 32*, 3363.
34. Martin, S. R., Teleman, A. A., Bayley, P. M., Drakenberg, T., and Forsén, S. (1992) *Eur. J. Biochem. 151*, 543.
35. Peersen, O. P., Madsen, T. S., and Falke, J. J. (1997) *Protein Sci. 6*, 794.
36. Tonomura, B., Nakatani, H., Ohnishi, M., Yamaguchi-Ito, J., and Hiromi, K. (1978) *Anal. Biochem. 84*, 370.
37. Tsien, R. Y., Pozzan, T., and Rink, T. J. (1982) *J. Cell Biol. 94*, 325.
38. Klotz, I. M. (1986) *Introduction to Biomolecular Energetics, Including Ligand-Receptor Interactions*, Academic Press, Orlando, FL.
39. Grabarek, Z., and Gergely, J. (1983) *J. Biol. Chem. 258*, 14103.
40. Gutfreund, H. (1995) *Kinetics for the Life Sciences*, Cambridge University Press, Cambridge.
41. White, H. D. (1988) *Biochemistry 27*, 3357.
42. Altenbach, C., and Seelig, J. (1984) *Biochemistry 23*, 3913.
43. Tocanne, J.-F., and Teissié, J. (1990) *Biochim. Biophys. Acta 1031*, 111.
44. Berridge, M. J. (1993) *Nature 361*, 315.
45. Means, A. R. (1994) *FEBS Lett. 347*, 1.
46. Clapham, D. E. (1995) *Cell 80*, 259.
47. Bootman, M. D., and Berridge, M. J. (1995) *Cell 83*, 675.
48. Linse, S., and Forsén, S. (1995) *Adv. Second Messenger Phosphoprotein Res. 30*, 89.
49. Falke, J. J. Drake, S. K. Hazard, A. L., and Peersen, O. B. (1994) *Q. Rev. Biophys. 27*, 219.
50. Swairjo, M. A., Concha, N. O., Kaetzel, J. R., and Seaton, B. A. (1995) *Nat. Sruct. Biol. 2*, 968.
51. Scott, D. L., White, S. P., Otwinowski, Z., Yuan, W., Gelb, M. H., and Sigler, P. B. (1990) *Science 250*, 1541.
52. Thunnissen, M. M. G. M., Ab, E., Kalk, K. H., Drenth, J., Dijkstra, B. W., Kuipers, O. P., Dijkman, R., de Haas, G. H., and Verheij, H. M. (1990) *Nature 347*, 689.
53. Ames, J. B., Tanaka, T., Ikura, M., and Stryer, L. (1995) *J. Biol. Chem. 270*, 30909.
54. Tanaka, T., Ames, J. B., Harvey, T. S., Stryer, L., and Ikura, M. (1995) *Nature 376*, 444.
55. Hughes, R. E., Brzovic, P. S., Klevit, R. E., and Hurley, J. B. (1995) *Biochemistry 34*, 11410.
56. Nalefski, E. A., McDonagh, T., Somers, W., Seehra, J., Falke, J. J., and Clark, J. D. (1997) Manuscript submitted for publication.

BI9717340